ELSEVIER

International Journal of Heat and Fluid Flow 21 (2000) 37–48

International Journal of HEAT AND FLUID FLOW

www.elsevier.com/locate/ijhff

Nonlinear eddy viscosity modelling for turbulence and heat transfer near wall and shear-free boundaries

K. Suga *, K. Abe [1]

Heat Transfer Laboratory, Toyota Central R & D Laboratories, Inc., Nagakute, Aichi 480-1192, Japan

Received 5 February 1999; accepted 17 August 1999

Abstract

New turbulence and turbulent heat flux models are proposed for capturing flow and thermal fields bounded by walls or free surfaces. The models are constructed using locally definable quantities only, without any recourse to topographical parameters. For the flow field, the proposed model is a cubic nonlinear k–ε–A three equation eddy viscosity model. It employs dependence on Lumley's stress flatness parameter A, by solving its modelled transport equation as the third variable. Since A vanishes at two-component turbulence boundaries, introducing its dependency enables a turbulence model to capture the structure of turbulence near shear-free surfaces as well as wall boundaries. To close the modelled A equation, an up-to-date second-moment closure is applied. For the thermal field, an explicit algebraic second-moment closure for turbulent heat flux is proposed. The new aspect of this heat flux model is the use of nonlinear Reynolds stress terms in the eddy diffusivity tensor. This model complies with the linearity and independence principles for passive scalar. The proposed models are tested in fully developed plane channel, open channel and plane Couette–Poiseuille flows at several fluid Prandtl numbers. The results show the very encouraging performance of the present proposals in capturing anisotropic turbulence and thermal fields near both wall and shear-free boundaries in the range of $0.025 \leqslant Pr \leqslant 95$.

Keywords: Turbulence model; Nonlinear eddy viscosity; Algebraic heat flux model; Wall bounded flow; Free surface flow

Notation

a_{ij}	anisotropic stress ($\equiv \overline{u_i u_j}/k - (2/3)\delta_{ij}$)
A	Lumley's stress flatness parameter
A_s	Lumley's stress flatness parameter, processed from the calculated strain field
A_2	the second invariant of anisotropic stress
k, k^+	turbulence energy (k/u_τ^2)
l	turbulent length scale ($\equiv k^{1.5}/\varepsilon$)
Pr	Prandtl number
Re	Reynolds number ($\equiv U_b\delta/\nu$)
R_t, $\widetilde{R}_t$	turbulent Reynolds number $[\equiv k^2/(\nu\varepsilon),\ k^2/(\nu\tilde{\varepsilon})]$
S_{ij}, $\tilde{S}$	$\equiv U_{i,j} + U_{j,i}, \tau\sqrt{S_{ij}S_{ij}/2}$
u_i, U_i	fluctuating and mean velocity components
u_τ	friction velocity
u'^+, v'^+, w'^+	$\sqrt{\overline{u^2}}/u_\tau, \sqrt{\overline{v^2}}/u_\tau, \sqrt{\overline{w^2}}/u_\tau$
$\overline{u_i u_j}$	Reynolds stress
U_b	bulk velocity
$\overline{u_i\theta}$, $\overline{u_i\theta}^+$	turbulent heat flux ($\overline{u_i\theta}/(u_\tau\overline{\Theta}_\tau)$)
x_i	coordinate direction
y^+	normalized wall normal distance ($\equiv u_\tau y/\nu$)
δ_{ij}	Kronecker's delta
ε, $\tilde{\varepsilon}$, ε^+	dissipation rate of k, $\varepsilon - 2\nu\sqrt{k}_{,k}\sqrt{k}_{,k}$, $\nu\varepsilon/u_\tau^4$
$\overline{\Theta}$, $\overline{\Theta}_\tau$, $\overline{\Theta}^+$	mean temperature, friction temperature, $\overline{\Theta}/\overline{\Theta}_\tau$
ν, ν_t	kinematic viscosity, kinematic eddy viscosity
τ	turbulent time scale ($\equiv k/\tilde{\varepsilon}$)
Ω_{ij}, $\tilde{\Omega}$	$\equiv U_{i,j} - U_{j,i}, \tau\sqrt{\Omega_{ij}\Omega_{ij}/2}$

1. Introduction

Working fluid in industrial machinery is usually bounded by walls, or in the case of liquid flow, one side of the flow may be open to gas. It is thus essential to estimate the flow and thermal quantities near the boundaries for designing fluid machines. To meet this, computational fluid dynamics has become an important tool and use of a turbulence model is now well established since most practical flows are turbulent.

For turbulent flow field, the most widely used turbulence model in industry is a linear eddy viscosity model (EVM) because of its numerical stability and low cost required.

* Corresponding author.
E-mail address: suga@flow.tytlabs.co.jp (K. Suga).
[1] Present address: Department of Aeronautics and Astronautics, Kyushu University, Fukuoka 812-8581, Japan.

0142-727X/00/$ - see front matter
PII: S0142-727X(99)00060-0

However, for capturing anisotropic stress fields, which affect the mean flow fields quite significantly, nonlinear terms are essential in the constitutive equation of an EVM. Most of the nonlinear EVMs have thus employed up to quadratic products of mean velocity gradient tensors (e.g. Speziale, 1987; Nisizima and Yoshizawa, 1987; Rubinstein and Barton, 1990; Myong and Kasagi, 1990). Several workers, however, have shown that cubic and even higher order terms appear in transforming an algebraic second-moment model to an explicit nonlinear EVM (e.g. Pope, 1975; Horiuti, 1990; Gatski and Speziale, 1993). Craft et al. (1993, 1996) pointed out that at least cubic terms were necessary to capture stream-line curvature (including swirling flows) effects in turbulent flows. Although their cubic nonlinear k–ε model improved predictions of such flow fields including impinging jets, it still predicted levels of the turbulence intensities with much too little difference among components in the buffer region of a boundary layer. They thus extended the model to a three equation nonlinear EVM by introducing an additional transport equation for the second anisotropic stress invariant, $A_2 \equiv a_{ij}a_{ji}$ (Suga, 1995; Craft et al., 1995, 1997). Since modern second-moment closures make some of their coefficients dependent on the stress invariants (e.g. Lumley, 1978; Launder and Tselepidakis, 1993; Craft and Launder, 1996), they employed a similar approach. Their three equation nonlinear eddy viscosity model, the CLS model hereafter, showed very encouraging results for predicting a wide range of wall-bounded flows including flows associated with turbomachinery (Chen et al., 1998a,b) and flows with shock/boundary layer interaction (Barakos and Drikakis, 1997).

However, on a shear-free boundary, such as a free surface and a moving shear-free wall of the Couette–Poiseuille flow, the usual linear or nonlinear stress–strain relations always return an isotropic stress field corresponding to the vanishing of the velocity gradients. Since the stress field is significantly anisotropic and reaches two-component turbulence at a shear-free boundary, capturing this anisotropic turbulence is crucial if the model is used to predict scalar diffusion processes near the boundary. Moreover, as Fig. 1(a) illustrates, when the eddy viscosity, ν_t, is estimated as $-\overline{uv}/U_{,y}$, the blocking effect on the normal fluctuating velocity results in significant damping on ν_t near a free surface ($y = \delta$) as well. No such an effect is, however, detected near the centerline of the plane channels. (Here, δ represents the channel half-width of a plane channel, the channel width of the plane Couette–Poiseuille flow, or the channel depth of an open channel.) Modelling this damping effect is generally difficult since local invariant parameters such as the turbulent Reynolds number do not vanish on free surfaces (Fig. 1(b)). Therefore, some ad hoc approaches have been proposed to treat free surface turbulent flows. Rodi (1980) corrected the length-scale near the surface through a modification to the boundary condition of ε using the distance from the surface. Celik and Rodi (1984) introduced a $\overline{v^2}$-damping function into the coefficient of the eddy viscosity: c_μ with the aid of an algebraic second-moment closure for $\overline{v^2}$.

Although as in Fig. 1(c), A_2 increases toward $\frac{2}{3}$ near a shear-free boundary, it is still hard to characterize shear-free turbulence with its behaviour. Thus, the CLS model also keeps the inherent weaknesses of the eddy viscosity modelling. Now, the presently focused parameter is Lumley's stress flatness parameter: $A \equiv 1 - \frac{9}{8}(A_2 - A_3), (A_3 \equiv a_{ij}a_{jk}a_{ki})$ (Lumley, 1978). Since it always vanishes in two-component turbulence as shown in Fig. 1(d), this feature is believed to be very useful to model turbulence near shear-free boundaries.

For capturing turbulence near walls and shear-free boundaries, it has been decided in the present study to solve a transport equation for A as the third variable to be coupled with the cubic nonlinear k–ε EVM. The present paper thus describes the derivation and the modelling strategy of the transport equation of A as well as the inclusion of its dependency in the cubic stress–strain relation.

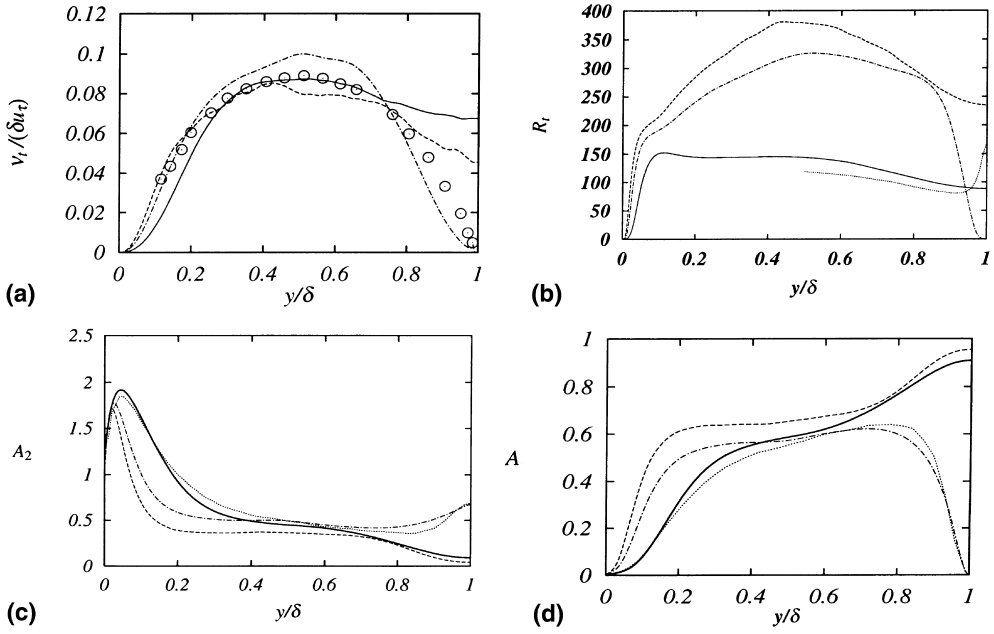

Fig. 1. Distributions of turbulent quantities: (a) eddy viscosity; (b) turbulent Reynolds number; (c) second stress invariant; (d) stress flatness parameter; ○ ○ ○: Open-channel, Nezu and Rodi (1986); ·····: Open-channel, (b) Handler et al. (1993), (c)(d) Lombardi et al. (1996); – · – · –: Couette–Poiseuille, Kuroda et al. (1995); ——: Channel at $Re = 2800$, Kim et al. (1987); – – –: Channel at $Re = 6875$, Kim (1990).

For turbulent thermal fields, algebraic expressions for turbulent heat flux have been widely used in engineering applications since they provide mean wall heat transfer rates at least with moderate satisfaction despite their simplicity. The most widely used algebraic approach is the eddy diffusivity modelling which employs some prescribed turbulent Prandtl number. However, in the case that individual normal stresses are reasonably predicted as in the present study, use of the Daly and Harlow (1970) generalized gradient-diffusion hypothesis (GGDH) arguably provides a more secure route for predicting the heat flux (e.g. Launder, 1988). The more elaborate but reliable algebraic approach may be the algebraic second-moment closure (Launder, 1975). Traditional *implicit* models derived from truncation of the convection and diffusion terms of the transport equation, however, sometimes lead to a stiff equation set that causes severe convergence difficulties. To avoid this stiffness problem, several *explicit* approaches have been recently proposed by inverting the matrix of the implicit equation set (Rogers et al., 1989; So and Sommer, 1995; Abe et al., 1996; Rhee and Sung, 1997).

Although many of these explicit algebraic models showed encouraging results, their predictive accuracy of the streamwise heat flux has a quite wide margin to be improved and some of them violate the linearity and independence principles set forth by Pope (1983). To satisfy these principles in forced convection regimes, it is required not to use coefficients dependent on turbulent scalar variables such as the temperature variance. Moreover, the model validations have usually been made against wall bounded flows, and thus their performance near shear-free interfaces is unknown.

Therefore, the present study focuses on the explicit approach of the algebraic second-moment closure for heat flux. In the derivation of the heat flux equations, the nonlinear stress–strain relation is extensively adapted and the effect of A is also introduced. The present heat flux model is thus designed to be applied to both wall and shear-free boundaries. The linearity and independence principles are also considered in the present model.

2. The proposed model for flow fields

2.1. The constitutive equation for $\overline{u_i u_j}$

The nonlinear constitutive relation used in this study is the cubic model of the CLS model.

$$\begin{aligned} a_{ij} \equiv \overline{u_i u_j}/k - \tfrac{2}{3}\delta_{ij} &= -c_\mu \tau S_{ij} + c_1\tau^2(S_{ik}S_{kj} - \tfrac{1}{3}S_{kl}S_{kl}\delta_{ij}) \\ &\quad + c_2\tau^2(\Omega_{ik}S_{kj} + \Omega_{jk}S_{ki}) + c_3\tau^2(\Omega_{ik}\Omega_{jk} - \tfrac{1}{3}\Omega_{lk}\Omega_{lk}\delta_{ij}) \\ &\quad + c_4\tau^3(S_{ki}\Omega_{lj} + S_{kj}\Omega_{li})S_{kl} + c_5\tau^3(\Omega_{il}\Omega_{lm}S_{mj} \\ &\quad + S_{il}\Omega_{lm}\Omega_{mj} - \tfrac{2}{3}S_{lm}\Omega_{mn}\Omega_{nl}\delta_{ij}) + c_6\tau^3 S_{ij}S_{kl}S_{kl} \\ &\quad + c_7\tau^3 S_{ij}\Omega_{kl}\Omega_{kl} + c_a A_{ij}, \end{aligned} \tag{1}$$

where the last term $c_a A_{ij}$ is an additional term introduced in this study to capture shear-free turbulence described later. The damping function of the eddy viscosity near a boundary may be divided into some parts corresponding to the factors which affect the eddy viscosity. Since A decreases near both wall and shear-free boundaries as $\nu_t(=c_\mu k\tau)$ does (see Fig. 1(a),(d)), the primary damping effect for c_μ can be expected to come from a function of A. However, the profile of A is affected by the Reynolds number, so some R_t effect may be still necessary in the damping. Strain dependency in c_μ is also required to keep the Reynolds stresses realizable at high strain rate cases since c_μ appears in the linear part of Eq. (1). Consequently, A, R_t and the strain invariant are considered as the damping factors in the present study. Accordingly, the coefficient c_μ may be expressed as:

$$c_\mu = 0.09 c_{\mu_A} c_{\mu_{R_t}} c_{\mu_S}. \tag{2}$$

By referring to a set of DNS data and considering the theoretical boundary limiting behaviour of ν_t, the sub-coefficients c_{μ_A}, $c_{\mu_{R_t}}$ and c_{μ_S} are modelled as:

$$\begin{aligned} c_{\mu_A} &= \min[1.05, 1.2\{1 - \exp(-A - (A/0.6)^\alpha)\} \\ &\quad + 0.18\{1 - \exp(-10A)\}^{1/2}], \end{aligned} \tag{3}$$

$$c_{\mu_{R_t}} = 1 + 2A\exp(-R_t^2/8100), \tag{4}$$

$$c_{\mu_S} = \min[1, 1.2/(1 + 0.06\eta)]. \tag{5}$$

Note that this empirical coefficient set is one of those which reproduce the DNS profiles with reasonably simple functional forms. The functions appearing in the coefficients are listed in Table 1.

The additional term A_{ij} is

$$A_{ij} = c_a'\tau^2(\sqrt{Ak}_{,i}\sqrt{Ak}_{,j} - \tfrac{1}{3}\delta_{ij}\sqrt{Ak}_{,k}\sqrt{Ak}_{,k}). \tag{6}$$

This term is designed to satisfy the limiting values at a shear-free boundary:

$$a_{11}(=c_a A_{11}) = a_{33} = \tfrac{1}{3}, \quad a_{22}(=c_a A_{22}) = -\tfrac{2}{3}.$$

Here, the index "2" denotes the direction normal to the boundary. Thus, the inclusion of this term enables an EVM to capture anisotropy of shear-free turbulence.

Corresponding to these modifications, the coefficients and functions in the cubic stress–strain relation: Eq. (1) are slightly modified from those of the CLS model as given in Table 1.

Table 1
The empirical coefficients in the cubic EVM

$c_1 = -0.05 f_q$	$c_2 = 0.11 f_q$	$c_3 = 0.42 f_q \dfrac{\tilde{S}}{\tilde{S}+\tilde{\Omega}}$	$c_4 = -0.8 f_c$	$c_5 = 0$	$c_6 = -0.5 f_c$	$c_7 = 0.5 f_c$
$\eta = \max(\tilde{S}, \tilde{\Omega}) r_\eta$		$\alpha = 1 + 2.6\min[1, R_t/200]$			$\beta = \min[10, \max(0, \tilde{S} - 5)]$	
$f_q = \dfrac{2/3 r_\eta^2 (1 - f_a)}{(1 + 1.8\eta)(1 + 0.0086\eta^2)^{1/2}}$		$f_c = \dfrac{(2/3) r_\eta^3}{(1 + 1.8\eta)(1 + 0.45\eta^{2.5})}$			$r_\eta = 1 + 0.9\{1 + 0.4\beta\exp(-\frac{R_t}{5})^{1/4}\} \times \exp\{-(\frac{A}{0.7})^2\}$	
$c_a = -(8/3)^{1/2} f_a / \{1 + 2(A_{ij}A_{ij})^{1/2}\}$		$c_a' = 1/\{1 - \exp(-\tilde{R}_t\}/30)$			$f_a = \exp\{-(\tilde{S}/2.2)^2\}$	

2.2. Modelling the transport equations

Deriving the exact transport equation for A is straightforward from its definition.

$$\frac{\mathrm{D}A}{\mathrm{D}t} = \underbrace{-\frac{9}{8k}\left(\frac{3}{2}A_3\mathscr{D}_{kk} + 2a_{ij}\mathscr{D}_{ij} - 3a_{jk}a_{ki}\mathscr{D}_{ij}\right)}_{\mathscr{D}_A} \underbrace{-\frac{9}{8k}\left(\frac{3}{2}A_3P_{kk} + 2a_{ij}P_{ij} - 3a_{jk}a_{ki}P_{ij}\right)}_{P_A} \underbrace{-\frac{9}{8k}\left(\frac{3}{2}A_3\Pi_{kk} + 2a_{ij}\Pi_{ij} - 3a_{jk}a_{ki}\Pi_{ij}\right)}_{\Pi_A} \underbrace{+\frac{9}{8k}\left(\frac{3}{2}A_3\varepsilon_{kk} + 2a_{ij}\varepsilon_{ij} - 3a_{jk}a_{ki}\varepsilon_{ij}\right)}_{\varepsilon_A}, \tag{7}$$

where $\mathscr{D}_{ij}, P_{ij}, \Pi_{ij}$ and ε_{ij} are, respectively, the diffusive transport, shear generation, pressure correlation, and dissipation rate of $\overline{u_iu_j}$. Amongst them, the shear generation term: $P_{ij} \equiv -(\overline{u_iu_k}U_{j,k} + \overline{u_ju_k}U_{i,k})$, needs no further approximation while in the present study, the recent second moment modelling is applied to the other terms.

Following Craft and Launder (1996) (the CL model hereafter), Π_{ij} is divided into two processes as:

$$\Pi_{ij} = \phi_{ij} + \frac{1}{2}\Pi_{kk}\frac{\overline{u_iu_j}}{k}, \tag{8}$$

where the pressure strain term is split into two parts: $\phi_{ij} = \phi_{ij1} + \phi_{ij2}$. Then, the cubic pressure strain model developed and widely tested at UMIST (see Craft and Launder, 1996) is adopted for ϕ_{ij1} and ϕ_{ij2}. After moderate algebra, the expression for the joint process of $P_A + \Pi_A$ reduces to:

$$P_A + \Pi_A = \frac{9\tilde{\varepsilon}}{8k}\left\{(\tilde{c_1} + f_{A2})(2A_2 - 3A_3) + \tilde{c_1}c_1'(2A_3 - 0.5A_2^2)\right\} + \frac{A}{k}\left\{0.45c_2'a_{ij}P_{ij} - (0.6 + 0.3c_2')P_{kk}\right\}. \tag{9}$$

Interestingly, the resultant form is considerably simple even though the cubic pressure strain model is adopted. Note that the terms including the second term in the right-hand side of Eq. (8) vanish in the algebraic process. Through the extensive test using the terms with c_2', we have found that their effect is fairly small in the present work and thus currently $c_2' = 0$ is adopted. The coefficients and functions are basically the same as those of the CL model though minor retuning is made for this study as listed in Table 2. The functions f_A and f_{A2} in Table 2 use A_s that is another stress flatness parameter simply processed from the calculated stress field. The use of A_s instead of A has been found to be better in the present model. Since $P_A + \Pi_A$ is the main source term of the A equation, it is desirable to have reasonable strain sensitivity in it. Furthermore, in the present modelling, A_2 is redefined as:

$$A_2 = A_3 + \tfrac{8}{9}(1 - A) \tag{10}$$

using A_3 and A obtainable from the stress field and the transport equation, respectively. This A_2 includes some transport effect and thus contributes to give smooth behaviour of $P_A + \Pi_A$.

The CL model introduced a new ε_{ij} form complying with the shear-free limit as well as the wall limit (Launder and Reynolds, 1983). After full consideration of their form, it has been found that the truncated form:

$$\varepsilon_{ij} = (1 - f_\varepsilon)\left(\varepsilon_{ij}' + \varepsilon_{ij}''\right)/D + \tfrac{2}{3}f_\varepsilon\varepsilon\delta_{ij} \tag{11}$$

might be enough in the present practice, where

$$\varepsilon_{ij}' = \left[2\nu f_\varepsilon' k_{,m}^{1/2}\left(k_{,i}^{1/2}\frac{\overline{u_ju_m}}{k} + k_{,j}^{1/2}\frac{\overline{u_iu_m}}{k}\right) + 2\nu f_\varepsilon' k_{,k}^{1/2}k_{,m}^{1/2}\frac{\overline{u_ku_m}}{k}\delta_{ij} + \frac{\overline{u_iu_j}}{k}\varepsilon\right],$$

$$\varepsilon_{ij}'' = \varepsilon\left(2\frac{\overline{u_ku_l}}{k}\,d_k^A\,d_l^A\delta_{ij} - \frac{\overline{u_iu_l}}{k}\,d_j^A\,d_l^A - \frac{\overline{u_ju_l}}{k}\,d_i^A\,d_l^A\right)f_R,$$

$$D = \frac{\varepsilon_{kk}' + \varepsilon_{kk}''}{2\varepsilon}.$$

Note that this form satisfies at least the wall limit. The ε_{ij}' term follows the CLS model while the ε_{ij}' term is introduced after the CL model with the *inhomogeneity indicators*:

$$d_i = \frac{N_i}{0.5 + (N_kN_k)^{1/2}}, \quad d_i^A = \frac{N_i^A}{0.5 + (N_k^AN_k^A)^{1/2}},$$

$$N_i = l_{,i}, \quad N_i^A = \left(lA^{1/2}\right)_{,i},$$

where $l = k^{1.5}/\varepsilon$. Thus, ε_A reduces to:

$$\varepsilon_A = -\frac{9}{8k}\left[(3A_3 - 2f_\varepsilon A_2)\varepsilon + \frac{(1 - f_\varepsilon)}{D}\left\{-3A_3\varepsilon + (\tfrac{16}{3} - 12A_2)\nu f_\varepsilon' a_{ij}k_{,i}^{1/2}k_{,j}^{1/2} - 4(A_2 + A_3)\nu f_\varepsilon' k_{,k}^{1/2}k_{,k}^{1/2} - f_R\varepsilon((3A_2 + \tfrac{8}{3})a_{ij}\,d_i^A\,d_j^A + (4A_2 - 2A_3)\,d_k^A\,d_k^A)\right\}\right], \tag{12}$$

$$D = 1 + \frac{5f_\varepsilon'\nu}{\varepsilon}(a_{ij}k_{,i}^{1/2}k_{,j}^{1/2} + \tfrac{2}{3}k_{,k}^{1/2}k_{,k}^{1/2}) + 2f_R(a_{ij}\,d_i^A\,d_j^A + \tfrac{2}{3}\,d_k^A\,d_k^A).$$

The empirical functions used are listed in Table 2. Note that those functions follow essentially the CLS and the CL models.

When the GGDH diffusion model of Daly and Harlow (1970) is applied to $\mathscr{D}_{ij}$, the $\mathscr{D}_A$ term reduces to:

$$\mathscr{D}_A = \left\{\left(\nu\delta_{kl} + c_s\overline{u_ku_l}\frac{k}{\varepsilon}\right)A_{,l}\right\}_{,k} + \frac{1}{k}\left(\nu\delta_{kl} + c_s\overline{u_ku_l}\frac{k}{\varepsilon}\right)(k_{,k}A_{,l} + k_{,l}A_{,k}) - \frac{9}{8}\left(\nu\delta_{kl} + c_s\overline{u_ku_l}\frac{k}{\varepsilon}\right)\left(6a_{ij}a_{jm,k}a_{mi,l} - 2a_{ij,k}a_{ij,l}\right). \tag{13}$$

Table 2
The coefficients in the A equation

$\tilde{c_1} = 3.1\min(A_2, 0.5)f_Af_{Rt}$	$c_1' = 1.1$	$c_2' = 0$
$f_{R_t} = \min(R_t/160, 1)$	$f_{A2} = A_s^3$	$f_R = (1 - A)\min\left[(R_t/80)^2, 1.0\right]$
$f_A = (A_s/14)^{1/2},\ A_s \leqslant 0.05$	$f_\varepsilon = A/0.15^{1/2},\ A \leqslant 0.15$	$f_\varepsilon' = \{1 - \exp(-R_t/5)\}^{1/2}$
$= A_s/0.7^{1/2},\ 0.05 < A_s < 0.7$	$= A^{1/2},\ 0.15 < A$	
$= A_s^{1/2}, = A_s \geqslant 0.7$		

Although no further approximation may be needed for this expression, it has been found that the turbulent part of the non-diffusive elements of the above form sometimes lead to an unstable solution. The following truncated form is thus used with $c_s = 0.22$.

$$\mathscr{D}_A = \left\{ \left(\nu\delta_{kl} + c_s\overline{u_k u_l}\frac{k}{\varepsilon} \right) A_{,l} \right\}_{,k} + \frac{\nu\delta_{kl}}{k}\left(k_{,k}A_{,l} + k_{,l}A_{,k}\right) - \frac{9}{8}\nu\delta_{kl}\left(6a_{ij}a_{jm,k}a_{mi,l} - 2a_{ij,k}a_{ij,l}\right). \tag{14}$$

For the k and $\tilde{\varepsilon}$ equations, the modelled equation set of the CLS model is used with some minor modifications following the CL model. They are: (1) the use of the pressure diffusion term in the k equation, and (2) the inclusion of an extra term in the $\tilde{\varepsilon}$ equation for a shear-free boundary. The detailed equation set is attached in Appendix A.

3. The proposed model for scalar fields

3.1. Algebraic turbulent heat flux modelling

With the assumption that the convection and the diffusion terms of $\overline{u_i\theta}$ are negligible compared with the other terms, the $\overline{u_i\theta}$ transport equation reduces to

$$0 = -\overline{u_i u_j}\,\overline{\Theta}_{,j} - \overline{u_j\theta}\,\overline{U}_{i,j} + \phi_{i\theta 1} + \phi_{i\theta 2}. \tag{15}$$

For the pressure-scalar correlation terms $\phi_{i\theta 1}$ and $\phi_{i\theta 2}$, many simple and complicated proposals can be found in the literature (Launder, 1976; Craft and Launder, 1991; etc.). Since all of the forms, however, may be expressed as:

$$\phi_{i\theta 1} + \phi_{i\theta 2} = c'_\theta\overline{u_i\theta} + M'_{ij}\overline{u_j\theta} + N'_{ij}\overline{\Theta}_{,j}, \tag{16}$$

introduction of Eq. (16) into Eq. (15) yields the following general algebraic expression:

$$\overline{u_i\theta} = M_{ij}\overline{u_j\theta} + N_{ij}\overline{\Theta}_{,j}, \tag{17}$$

where M's and N's are tensors consisting of the Reynolds stress tensor and mean velocity gradient tensors: S_{ij} and Ω_{ij}. Eq. (17) implicitly includes the heat flux tensor on both the left- and right-hand sides and this sometimes makes numerical solutions unstable.

Eq. (17) may be modified to

$$\left(\delta_{ij} - M_{ij}\right)\overline{u_j\theta} = N_{ij}\overline{\Theta}_{,j}. \tag{18}$$

The inversion of this matrix equation gives an explicit algebraic form. The resultant form may be written using k, τ and a coefficient c_θ as:

$$\overline{u_i\theta} = -c_\theta k\tau O_{ij}\overline{\Theta}_{,j}, \tag{19}$$

where O_{ij} also consists of the Reynolds stress and mean velocity gradient tensors. This form is essentially the gradient diffusion model. (This approach was originally presented by Rogers et al. (1989).) In the present study, the eddy diffusivity tensor O_{ij} is split into σ_{ij} and α_{ij} which are, respectively, the symmetric and the asymmetric parts.

$$\overline{u_i\theta} = -c_\theta k\tau\left(\sigma_{ij} + \alpha_{ij}\right)\overline{\Theta}_{,j}. \tag{20}$$

Here, it is assumed that the Reynolds stresses can be expanded in terms of the mean velocity gradient tensors. The most general expansion originally used in the nonlinear eddy viscosity approach of Pope (1975) allows one to express a_{ij} as:

$$a_{ij} = \sum_{\lambda=1}^{10} G^\lambda T^\lambda_{ij}, \tag{21}$$

where T^λ_{ij} is a symmetric tensor composed of S_{ij} and Ω_{ij} and the coefficients G^λ's include invariant functions. Note that the right-hand side of the above equation has 10 elements and no further independent element is necessary by the Cayley–Hamilton theorem. By the use of this equation, the Reynolds stress tensor in σ_{ij} is replaced and the resultant form of σ_{ij} is written in a series of tensors composed of S_{ij} and Ω_{ij}. It is in fact the same as Eq. (21) with its own series of the coefficients G^λ. Since the higher order products: $a_{il}a_{lj}$ and $a_{il}a_{lk}a_{kj}$, etc., may be also written in the same form as Eq. (21), T^λ_{ij} can be expressed with a series of products of the Reynolds stress tensor. However, the higher order products than the quadratic order may be rewritten with lower order terms by the Cayley–Hamilton theorem and thus the resultant generally expanded form for σ_{ij} is simply

$$\sigma_{ij} = c'_{\sigma 0}\delta_{ij} + c'_{\sigma 1}a_{ij} + c'_{\sigma 2}a_{il}a_{lj},$$

or

$$\sigma_{ij} = c_{\sigma 0}\delta_{ij} + c_{\sigma 1}\overline{u_i u_j}/k + c_{\sigma 2}\overline{u_i u_l}\,\overline{u_l u_j}/k^2. \tag{22}$$

In this form, the term $c_{\sigma 0}\delta_{ij}$ corresponds to the model with a turbulent Prandtl number while $c_{\sigma 1}\overline{u_i u_j}/k$ corresponds to the GGDH model. Eq. (22) further includes the quadratic term and thus it is similar to the form previously discussed by Abe and Suga (1998). Since a weak contribution of asymmetric terms is considered to be useful, the following form is considered in the present study though the most general asymmetric form includes much more terms.

$$\alpha_{ij} = c_{\alpha 0}\tau\Omega_{ij} + c_{\alpha 1}\tau\left(\Omega_{il}\overline{u_l u_j}/k + \Omega_{lj}\overline{u_i u_l}/k\right). \tag{23}$$

3.2. Optimization of the model coefficients

In the modelling process for the coefficients, the boundary limiting behaviour of turbulent quantities is considered. With the basic analyses as in Appendix B, heat flux components behave as

$$\overline{u\theta} \propto O(y^2), \overline{v\theta} \propto O(y^3) : \text{constant wall temperature}, \tag{24}$$

$$\overline{u\theta} \propto O(y^1), \overline{v\theta} \propto O(y^2) : \text{constant wall heat flux}, \tag{25}$$

$$\overline{u\theta} \propto O(y^0), \overline{v\theta} \propto O(y^1) : \text{near free-surface}. \tag{26}$$

Now, two-dimensional field is considered for simplicity. The present model expression, Eqs. (20)–(23), in two-dimensional fields gives

$$\begin{aligned} \overline{u\theta} &= -c_\theta k\tau\{\sigma_{11}\overline{\Theta}_{,1} + (\sigma_{12} + \alpha_{12})\overline{\Theta}_{,2}\}, \\ \overline{v\theta} &= -c_\theta k\tau\{(\sigma_{12} - \alpha_{12})\overline{\Theta}_{,1} + \sigma_{22}\overline{\Theta}_{,2}\}, \end{aligned} \tag{27}$$

and each tensor component is expressed as

$$\begin{aligned} \sigma_{11} &= c_{\sigma 0} + c_{\sigma 1}\overline{u^2}/k + c_{\sigma 2}(\overline{u^2}^2 + \overline{uv}^2)/k^2, \\ \sigma_{22} &= c_{\sigma 0} + c_{\sigma 1}\overline{v^2}/k + c_{\sigma 2}(\overline{uv}^2 + \overline{v^2}^2)/k^2, \\ \sigma_{12} &= c_{\sigma 1}\overline{uv}/k + c_{\sigma 2}\overline{uv}(\overline{u^2} + \overline{v^2})/k^2, \\ \alpha_{12} &= c_{\alpha 0}\tau\Omega_{12} + c_{\alpha 1}\tau\Omega_{12}(\overline{v^2}/k + \overline{u^2}/k), \end{aligned} \tag{28}$$

where the indexes "1" and "2" denote the streamwise direction and the direction normal to the boundary, respectively. Considering the above algebraic expressions, the requirements for the model coefficients are found as follows. Firstly, the contribution from the asymmetric tensor α_{ij} is assumed to be small. Then, due to the well-known anomaly of the model with a turbulent Prandtl number, which hardly predicts the

streamwise heat flux, the corresponding coefficient is set at zero $c_{\sigma 0} = 0$. In the case of a fully developed plane channel flow with different constant wall temperatures, the streamwise temperature gradient vanishes. In this particular condition, Eqs. (27) and (28) give the following condition for satisfying the requirement of Eq. (24).

$$c_\theta (c_{\sigma 1} + c_{\sigma 2}) \propto \mathrm{O}(y^{-1}). \tag{29}$$

According to the conclusion of Abe and Suga (1998), the model performance should be expected mainly from the quadratic term in σ_{ij} but the effect of the linear term is important for low Pr cases and near shear-free boundaries. Thus, the coefficient $c_{\sigma 1}$ needs to be weighted near a free surface. To meet the requirement of Eq. (26), the following condition may be derived for a fully developed open channel flow.

$$c_\theta c_{\sigma 1} \propto \mathrm{O}(y^{-1}). \tag{30}$$

In the present study, the following conditions are chosen to satisfy Eqs. (29) and (30) though there are many other options.

$$c_\theta \propto \mathrm{O}(y^{-1}), \quad c_{\sigma 1}, c_{\sigma 2} \propto \mathrm{O}(y^0). \tag{31}$$

These conditions also enable the model to satisfy Eq. (25) when a fully developed plane channel flow with constant wall heat flux is considered.

Considering Eq. (31) as well as the conclusion of Abe and Suga (1998), we have performed numerical experiments using the DNS and LES databases. The resultant set of optimized model coefficients is

$$\begin{aligned}
c_\theta &= \frac{0.4}{\left\{1 - \exp[-(A/0.05)^2]\right\}^{1/4}},\\
c_{\sigma 0} &= 0,\\
c_{\sigma 1} &= 0.15 f_\mathrm{b} + 0.1 f_{Pr},\\
c_{\sigma 2} &= 1 - f_\mathrm{b} - f_{Pr},\\
c_{\alpha 0} &= 0,\\
c_{\alpha 1} &= (1 - f_{Pr})\left\{\frac{-0.5A\xi}{1+\xi^2} - \frac{0.02}{A + (\xi + 0.2)^2}\exp\left[-(\xi/2.2)^2\right]\right\},\\
f_\mathrm{b} &= (1 - f_{Pr})^2 \exp[-\xi - (A/0.6)^2],\\
f_{Pr} &= \frac{1}{1 + (Pr/0.085)^{1.5}},\\
\xi &= \tilde{S}.
\end{aligned} \tag{32}$$

The shear-free effects and Prandtl number effects are included by employing the weighting functions f_b and f_{Pr}, respectively. Due to the inclusion of A dependency, f_b is especially sensitized to the two-component turbulence. This set of coefficients satisfies the linearity and independence principles for passive scalar due to the elimination of scalar field variables. (Currently, the term with $c_{\alpha 0}$ is not used in the present model.)

The proposed set of coefficients is also effective if an anisotropic turbulent flow field is well captured by a full second moment closure or another nonlinear EVM. However, when the distribution of A is not reasonably given, particularly near a boundary, the model performance is not fully expected since some of the model coefficients utilize the boundary limiting behaviour of A: $A \propto \mathrm{O}(y^2)$. Thus, another set of coefficients is given in Appendix C for a turbulence model which does not provide such a boundary limiting behaviour of A. Note that the coefficients listed in Appendix C are only effective for wall shear flow cases not for shear-free boundary layers because the dependency on A is excluded from them.

4. Applications and discussions

In order to validate their performance in shear-free turbulence, the proposed models have been tested in a fully developed open channel flow and a plane Couette–Poiseuille flow without shear on the moving wall, as well as for plane channel flows. The parabolic computations have been performed using the PASSABLE code (Leschziner, 1982). The computational domain extends from the symmetry plane or the shear-free boundary to the wall with 100 grid nodes distributed nonuniformly with a concentration near the boundaries. The grid distribution was adjusted for each test case to ensure grid independency of the solution. Also, the solutions were confirmed to be grid independent by comparing with results on much finer grids. The mean momentum equation coupled with the k, ε and A transport equations for turbulence has been computed. With the resultant flow quantities, the mean temperature transport equation has been computed with the present algebraic heat flux model.

4.1. Flow field predictions

The specific boundary conditions used for shear free regions ($y = \delta$) are listed in Table 3. Fig. 2 shows satisfactory agreement between the predicted mean velocity profiles and the DNS data. (Note that the DNS of the plane Couette–Poiseuille flow by Kuroda et al., 1995 is not perfectly shear-free at the moving wall though the shear is very small.) The predicted turbulent shear stress distributions agree quite well with the DNS results as shown in Fig. 3. Fig. 4 compares the predicted root mean square values of the Reynolds normal stresses with the DNS results. The stress profile in the shear-free region is very different for the three test cases though the strain field is nearly the same in all cases. The agreement between the prediction and the DNS data is fairly satisfactory for all components in each flow. Particularly, the present model successfully demonstrates its ability to capture the characteristic behaviour of the Reynolds normal stresses near the free surface where only the component normal to the surface vanishes. This confirms that the proposed stress–strain relation is also effective for shear-free turbulence.

Fig. 5 compares the predicted stress flatness parameters with the DNS results. Although the agreement is generally satisfactory, values in the core regions are underpredicted. This is partly because of the truncation made in Eq. (14). (Adopting Eq. (13) made the agreement closer.) According to the predicted behaviour of A which produces the primary damping effect on ν_t in the present model, the predicted eddy viscosity behaves reasonably near both wall and shear-free boundaries as shown in Fig. 6. (Obviously, further refinements are necessary.)

The predicted dissipation rate is also satisfactory as shown in Fig. 7 which compares the prediction and the DNS data of Kuroda et al. (1995). The agreement near both shear and shear free walls implies that the present ε equation is fairly successful in capturing the dissipation rate in two-component turbulence.

Table 3
The flow field boundary conditions used at $y = \delta$

Flow case	U	k	$\tilde{\varepsilon}$	A
Plane channel	$U_{,y} = 0$	$k_{,y} = 0$	$\tilde{\varepsilon}_{,y} = 0$	$A_{,y} = 0$
Open channel	$U_{,y} = 0$	$k_{,y} = 0$	$\tilde{\varepsilon}_{,y} = 0$	$A = 0$
Couette–Poiseuille	$U_{,y} = 0$	$k = 0$	$\tilde{\varepsilon} = 0$	$A = 0$

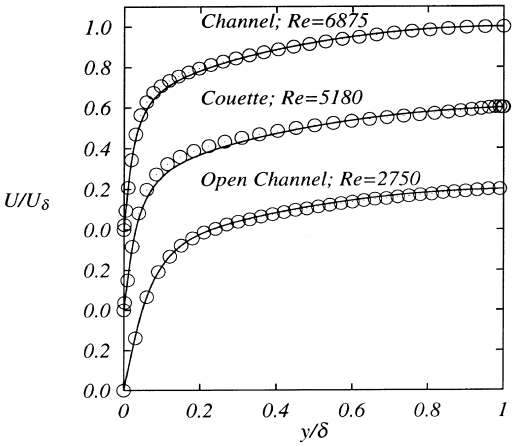

Fig. 2. Mean velocity distributions; symbols: DNS, channel: Kim et al. (1987), Kim (1990); Couette–Poiseuille: Kuroda et al. (1995); open channel: Lombardi et al. (1996); lines: present model.

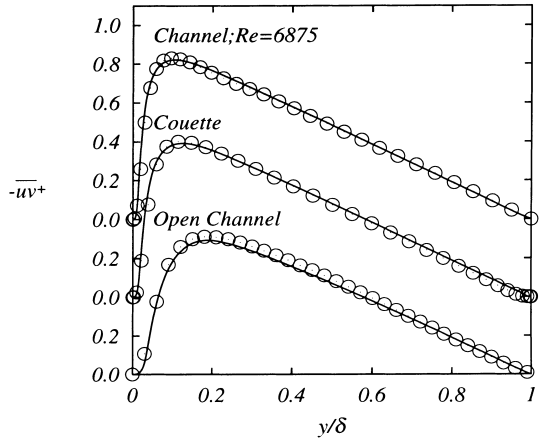

Fig. 3. Turbulent shear stress distributions; key as Fig. 2.

4.2. Thermal field predictions

Fig. 8 shows the comparison between the present predictions and the DNS and the LES results of fully developed thermal fields of plane channels. The fluid Prandtl number ranges from 0.025 to 7.0. A constant wall temperature condition and internal heat source are imposed for all cases except for the case of $Pr = 0.025$ which assumes constant wall heat flux. These boundary conditions are consistent with those of the simulations. Generally, excellent agreement can be seen in the distributions of the normalized mean temperature $\overline{\Theta}$ and heat flux components, $\overline{u\theta}$ and $\overline{v\theta}$. Although the presently predicted $\overline{u\theta}$ does not perfectly accord with the data in the core region around $y/\delta = 0.2$, in the higher Pr cases, the general profiles and the peak values are well captured. This is due to the inclusion of quadratic terms in the heat flux model as well as the reasonable prediction of the Reynolds stresses (shown in Fig. 4). An improvement to the underprediction around $y/\delta = 0.2$ would be made by modifying the asymmetric tensor α_{ij} since linear and quadratic terms of σ_{ij} produce larger ratio of $\overline{v\theta}/\overline{u\theta}$ in the core region at high Pr number (see Abe and Suga, 1998). Note that no previously proposed explicit algebraic model could capture this peak values with comparable accuracy to the present results, as shown in Fig. 9.

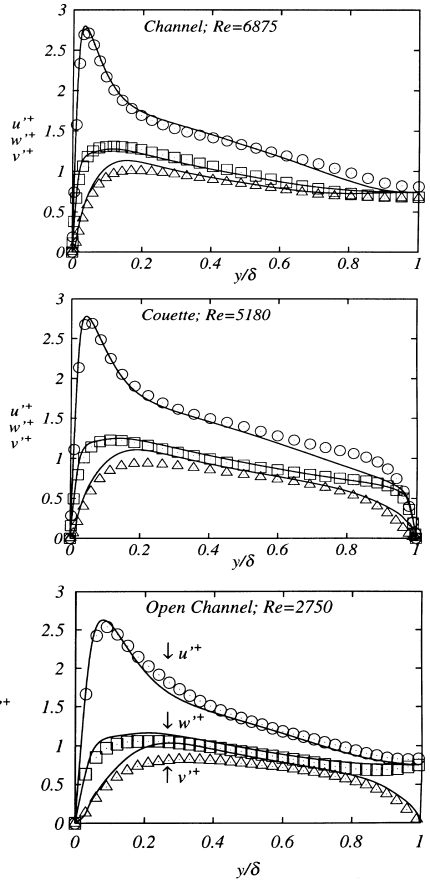

Fig. 4. Turbulent intensities; key as Fig. 2.

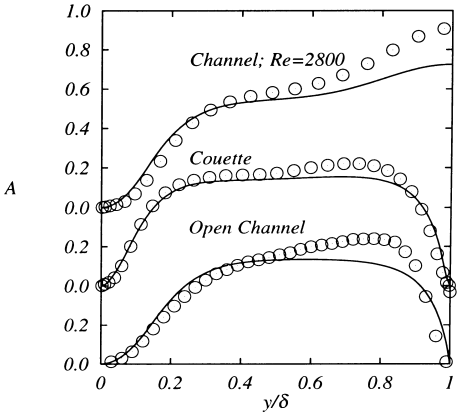

Fig. 5. Stress flatness parameter distributions; key as Fig. 2.

Similar tendencies can be seen in Fig. 10 which compares the results of the thermal fields with the "wall transfer" thermal boundary condition of Rogers et al. (1989). In this condition, there is a temperature difference between the two walls facing each other. The agreement is also generally sufficient.

In Fig. 11, the predicted results by the LES and present computations of a fully developed open channel water flow are compared. In the computation, constant heat flux conditions are imposed on both the wall and the free surface. Reasonably

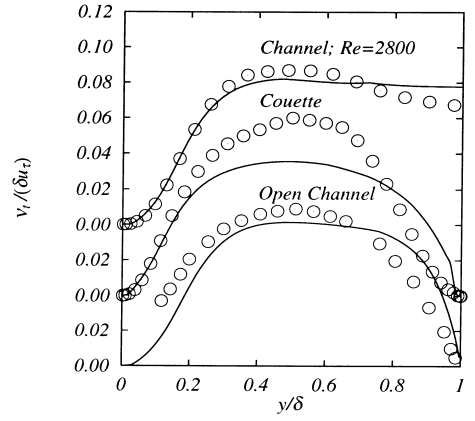

Fig. 6. Eddy viscosity distributions; symbols: data as in Fig. 1(a); lines: present model.

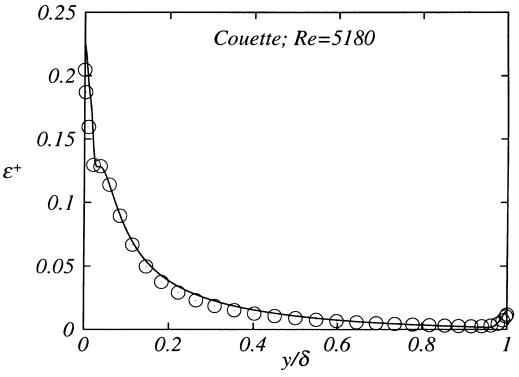

Fig. 7. Turbulent dissipation rate in the Couette–Poiseuille flow; key as Fig. 2.

satisfactory agreement can be seen in the mean temperature and $\overline{v\theta}$ distributions. The present heat flux model reproduces generally a reasonable distribution of $\overline{u\theta}$ of the LES though the agreement is not perfect. In fact, the present model does give a good level of $\overline{u\theta}$ near the shear-free surface which has been very difficult in principle to predict with previous proposals in the literature. This success comes from a combination of the linear terms in Eq. (22) and the satisfactory flow field prediction given by the k–ε–A model. The poor agreement in $\overline{u\theta}$ near the free surface, however, partly corresponds to the poor predictive accuracy of A there. Due to the slight overprediction of A in the vicinity of the free surface (see Fig. 5), the designed performance of the weighting function f_b for free surfaces is not fully obtained.

Fig. 11 also compares the results of the Couette–Poiseuille flow with a moving shear-free wall. The thermally imposed boundary condition is the "wall transfer" condition. Although the tendency in the mean temperature is similar to that of the open channel, a clear difference can be seen in the behaviour of $\overline{u\theta}$ near the shear-free boundaries ($y/\delta = 1$). (While they look similar to each other, the limiting behaviour of the predicted $\overline{v\theta}$ near shear-free boundaries is also different as discussed in the former section.) The present model does successfully predict this discrepancy though further refinements seem to be needed.

Fig. 12 compares the mean temperature distributions of the present heat flux model and the experiments of Neumann (1968) for an engineering-oil flow where $Pr = 95$. The experimental correlation proposed by Kader (1981) is also plotted in the figure for comparison. The presented agreement is satisfactory and thus it can be said that the present model is applicable to Prandtl numbers at least up to the above value.

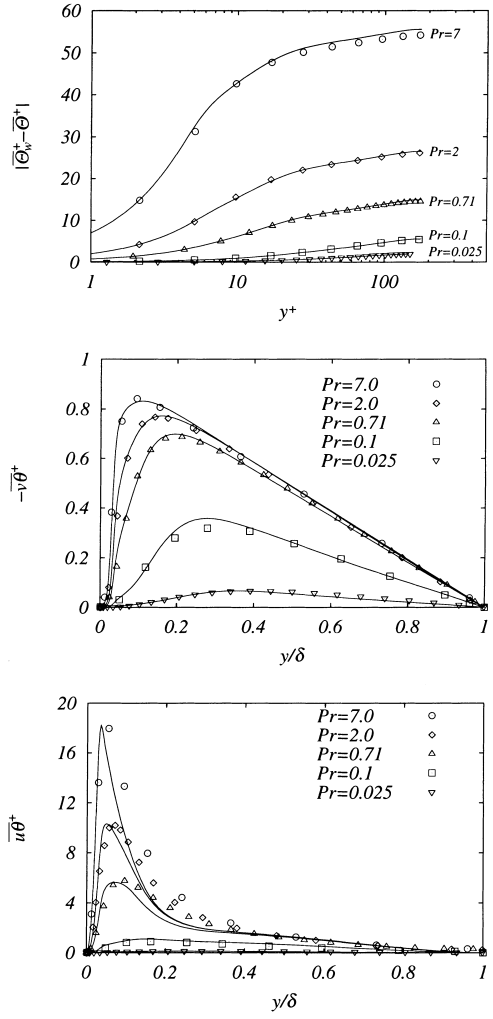

Fig. 8. Turbulent thermal fields in plane channels with internal heat source at $Re = 2800$; ———: present model; symbols: DNS/LES, $Pr = 7$: Abe and Suga (1998), $Pr = 2, 0.1$: Kim and Moin (1989), $Pr = 0.71$: Horiuti (1993), $Pr = 0.025$, (constant wall heat flux condition at $Re = 2280$): Kasagi and Ohtsubo (1993).

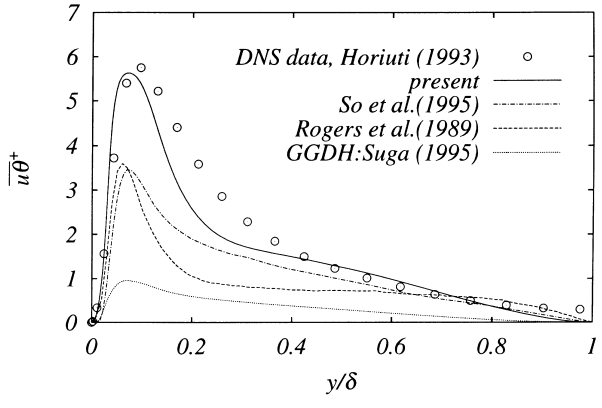

Fig. 9. Comparison in the predicted streamwise turbulent heat flux in a plane channel at $Re = 2800$, $Pr = 0.71$.

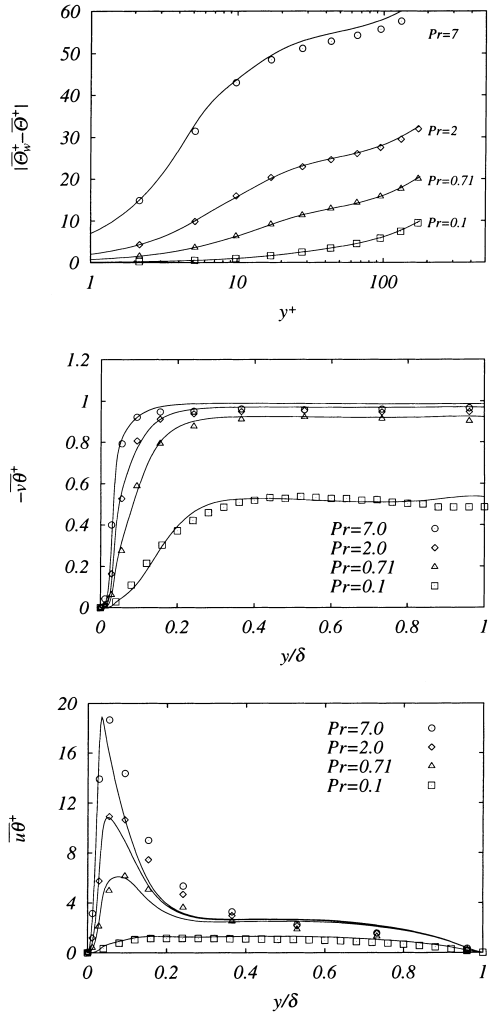

Fig. 10. Turbulent thermal fields in plane channels with wall transfer at $Re = 2800$; ——: present model; symbols: DNS/LES, ($Pr = 7, 2, 0.71$): Abe and Suga (1998); ($Pr = 0.1$): Rogers et al. (1989).

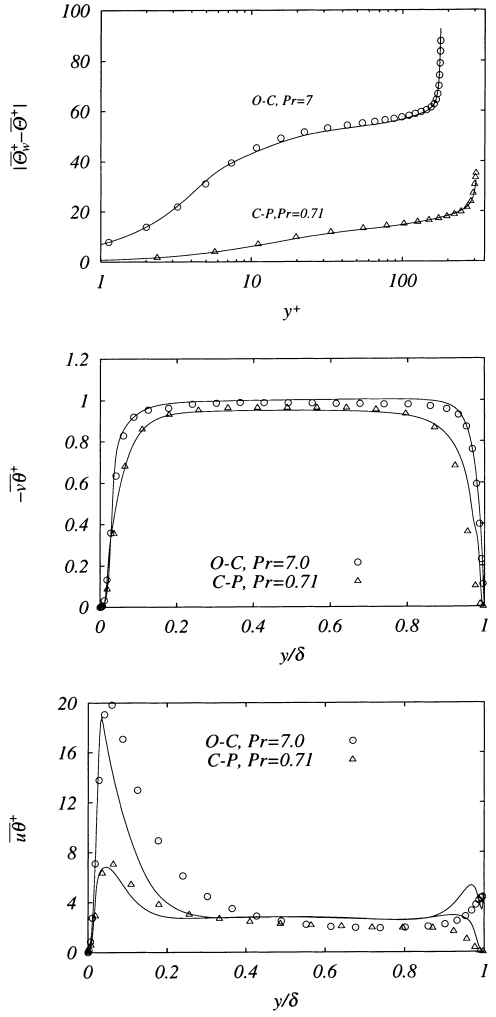

Fig. 11. Turbulent thermal fields in an open channel, O-C, ($Re = 2800$) and Couette–Poiseuille, C–P, ($Re = 5180$) flows; ——: present model; symbols: Abe and Suga (1998).

5. Concluding remarks

This paper has presented the development of a new cubic nonlinear k–ε–A three equation EVM and a new explicit algebraic scalar-flux model for passive scalar. They are designed to handle anisotropic turbulence and heat transfer phenomena, especially that near a two-component turbulence boundary. The features that distinguish the present work from the previous contributions are

1. the introduction of the transport effects of the stress flatness parameter, A, which enables the nonlinear EVM to capture the characteristics of two-component turbulence and makes the model free from topography;
2. the closure of the transport equation of A using the latest second-moment closure; and
3. the derivation of an explicit algebraic heat flux model that includes contribution from the quadratic products of the Reynolds stress tensor.

Since A always vanishes at two-component turbulence boundaries, the introduction of its dependence successfully enables the nonlinear EVM and the heat flux model to capture the characteristics of wall and shear-free turbulence.

The application results show the models' excellent performance to predict anisotropic turbulent flow and thermal fields

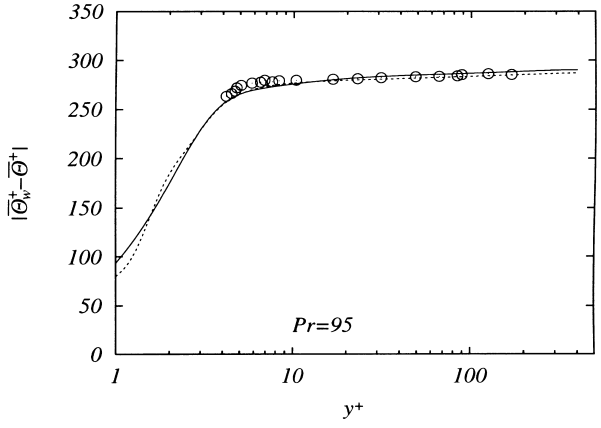

Fig. 12. Mean temperature distribution in an engineering oil flow ($Pr = 95$) at $Re = 7000$; ○ ○ ○: experiments, Neumann (1968); ——: present model; . . . . . .: experimental correlation, Kader (1981).

in the range of $0.025 \leqslant Pr \leqslant 95$. Moderate defects in the models, however, have been pointed out. They are the underprediction of A and the streamwise heat flux in the core region of a channel, and the overprediction of the streamwise heat flux

near a shear-free surface (which corresponds to the poor predictive accuracy of A there). Therefore, further work is necessary for improving the model of the A equation as well as the heat flux model in the core region. It is also necessary to validate the present proposals in more complex flow fields. (Although a detailed discussion is currently underway, some encouraging results have been obtained in a three-dimensional duct flow and a flow around a bluff body. Those results will be presented elsewhere.)

Acknowledgements

KS thanks Prof. B.E. Launder and Dr. T.J. Craft of UMIST for their fruitful suggestions. The original idea for developing a model with a transport equation of A came from the discussion with Prof. Launder while KS was studying at UMIST.

Appendix A. The k and $\tilde{\varepsilon}$ equations

The transport equation for k is:

$$\frac{\mathrm{D}k}{\mathrm{D}t} = \left\{ \left(\nu\delta_{kl} + 0.22\overline{u_k u_l}\frac{k}{\varepsilon} \right) k_{,l} \right\}_{,k} + \Pi_k + P_k - \varepsilon, \tag{A.1}$$

where

$$\Pi_k = \frac{1}{2}\Big[\left(0.35 d_k + 0.77 d_k^4\right) (\nu\varepsilon A A_2 k)^{1/2} \Big\{ c_{pd1} A_2 + 0.4 R_\mathrm{t}^{-1/4} \exp\left(-R_\mathrm{t}/40\right) \Big\} \Big]_{,k}, \tag{A.2}$$

$$c_{pd1} = 1 + 2\exp(-R_\mathrm{t}/40).$$

The transport equation for $\tilde{\varepsilon}$ is:

$$\frac{\mathrm{D}\tilde{\varepsilon}}{\mathrm{D}t} = \left\{ \left(\nu\delta_{kl} + 0.18\overline{u_k u_l}\frac{k}{\varepsilon} \right) \tilde{\varepsilon}_{,l} \right\}_{,k} + c_{\varepsilon 1} P_k \frac{\tilde{\varepsilon}}{k} - c_{\varepsilon 2}\frac{\tilde{\varepsilon}^2}{k} + P_{\varepsilon 3} + S_{\varepsilon 1} + S_{\varepsilon 2}, \tag{A.3}$$

where

$$P_{\varepsilon 3} = 1.3\,\nu\nu_\mathrm{t} U_{i,kj} U_{i,kj} + \nu\frac{\nu_\mathrm{t}}{k} k_{,k} U_{i,l} U_{i,kl}, \tag{A.4}$$

and the coefficients are listed in Table 4. The additional term $S_{\varepsilon 1}$ is modified from the term in the CL model which is designed for a shear-free boundary.

$$S_{\varepsilon 1} = (1-A)\tilde{\varepsilon}(c_\mu A k)^{1/2} A_{,k} (l A^{1/2})_{,k}. \tag{A.5}$$

Another additional term is introduced to balance the viscous diffusion.

$$S_{\varepsilon 2} = -(\varepsilon - \tilde{\varepsilon})(\tilde{\varepsilon} - P_k)/k. \tag{A.6}$$

Note that a further term composed of some length-scale gradients as in the CLS model should be involved when applications for impinging flows are considered.

Table 4
The coefficients in the $\tilde{\varepsilon}$ equation

$c_{\varepsilon 1} = 1.0 + 0.15(1 - A^{1/2})$	$c_{\varepsilon 2} = 1.92/(1 + 0.7 A_d A_2^{1/2})$	$A_d = \max[0.2, A](R_\mathrm{t}/20)^2/\{1 + (R_\mathrm{t}/20)^2\}$

Appendix B. Boundary limiting behaviour

In the case that U corresponds to the streamwise velocity component, the analytical limiting behaviour of turbulent quantities is:

$$\text{near-wall}\begin{cases} U_{,y} \propto \mathrm{O}(y^0) : \text{with shear}, \\ U_{,y} \propto \mathrm{O}(y^1) : \text{without shear}, \\ u, w \propto \mathrm{O}(y), \quad v \propto \mathrm{O}(y^2), \\ k, \tilde{\varepsilon}, \overline{u^2}, \overline{w^2} \propto \mathrm{O}(y^2), \\ \overline{v^2} \propto \mathrm{O}(y^4), \quad \overline{uv} \propto \mathrm{O}(y^3), \\ \theta \propto \mathrm{O}(y) : \text{constant wall temperature}, \\ \theta \propto \mathrm{O}(y^0) : \text{constant wall heat flux}, \end{cases}$$

$$\text{free surface}\begin{cases} U_{,y} \propto \mathrm{O}(y^1), \\ u, w \propto \mathrm{O}(y^0), \quad v \propto \mathrm{O}(y), \\ k, \tilde{\varepsilon}, \overline{u^2}, \overline{w^2} \propto \mathrm{O}(y^0), \\ \overline{v^2} \propto \mathrm{O}(y^2), \quad \overline{uv} \propto \mathrm{O}(y^1), \\ \theta \propto \mathrm{O}(y^0), \end{cases} \tag{B.1}$$

where y is the distance from the boundary. In two-dimensional flow fields, after a moderate amount of algebra, the definition of A reduces to

$$A = \frac{27}{8}\frac{\overline{w^2}}{k^3}\left(\overline{u^2}\;\overline{v^2} - \overline{uv}^2 \right), \tag{B.2}$$

and thus its theoretical behaviour is $A \propto \mathrm{O}(y^2)$ near both walls and free surfaces.

Appendix C. Another set of coefficients for the heat flux model

The presently proposed heat flux model (Eqs. (20)–(23)) can be also combined with the other nonlinear EVMs or second-moment closures. In the case that the distribution of A is not captured reasonably, the following set of modified coefficients may be used instead of Eq. (32).

$$\begin{aligned} c_\theta &= \frac{0.38}{\{1 - \exp(-R_\mathrm{t}/100)\}^{1/4}}, \\ c_{\sigma 0} &= 0, \\ c_{\sigma 1} &= 0.2 f_\mathrm{b} + 0.1 f_{Pr}, \\ c_{\sigma 2} &= 1 - f_\mathrm{b} - f_{Pr}, \\ c_{\alpha 0} &= 0, \\ c_{\alpha 1} &= (1 - f_{Pr})\left\{ \frac{-0.5 g_A \xi}{1 + 5\xi^2} - \frac{0.02}{g_A + (\xi + 0.2)^2}\exp\left[-(\xi/2.2)^2 \right] \right\}, \\ f_\mathrm{b} &= (1 - f_{Pr})^2 \exp[-(\xi/2.2)^2 - (g_A/0.3)^2], \\ f_{Pr} &= \frac{1}{1 + (Pr/0.085)^{1.5}}, \\ g_A &= 0.3\left[1 - \exp\left\{ -(R_\mathrm{t}/70)^2 \right\} \right], \\ \xi &= S, \end{aligned} \tag{C.1}$$

where

$$\tau = f_t k/\varepsilon, \quad f_t = [1 - \exp\left\{ - (R_t/70)^{1/2} \right\}]^{-1} \quad \text{and}$$

$$S \equiv \tau\sqrt{S_{ij}S_{ij}/2}.$$

The predictive performance with this set is comparable to the presented results using Eq. (32), though it is limited only in wall shear flow cases.

References

Abe, K., Kondoh, T., Nagano, Y., 1996. A two-equation heat transfer model reflecting second-moment closures for wall and free turbulent flows. Int. J. Heat Fluid Flow 17, 228–237.

Abe, K., Suga, K., 1998. Large eddy simulation of passive scalar fields under several strain conditions. Proc. Turbulent Heat Transfer 2, Manchester, 8.15–8.30.

Barakos, G., Drikakis, D., 1997. Validation of linear and non-linear low-Re turbulence models in shock/boundary layer interaction. In: Proceedings of the 11th Symposium on Turbulent Shear Flows. Grenoble, pp. 32.19–32.24.

Celik, I., Rodi, W., 1984. Simulation of free-surface effects in turbulent channel flows. Physicochem. Hydrodyn. 5, 217–227.

Chen, W.L., Lien, F.S., Leschziner, M.A., 1998a. Non-linear eddy viscosity modelling of transitional boundary layers pertinent to turbomachine aerodynamics. Int. J. Heat Fluid Flow 19, 297–306.

Chen, W.L., Lien, F.S., Leschziner, M.A., 1998b. Computational prediction of flow around highly loaded compressor-cascade blades with non-linear eddy viscosity models. Int. J. Heat Fluid Flow 19, 307–319.

Craft, T.J., Launder, B.E., 1991. Computation of impinging flows using second-moment closures. In: Proceedings of the Eighth Symposium on Turbulent Shear Flows, Munich, paper 8-5.

Craft, T.J., Launder, B.E., 1996. A Reynolds-stress closure designed for complex geometries. Int. J. Heat Fluid Flow 17, 245–254.

Craft, T.J., Launder, B.E., Suga, K., 1993. Extending the applicability of eddy viscosity models through the use of deformation invariants and non-linear elements. In: Proceedings of the Fifth International Symposium on Refined Flow Modelling and Turbulence Measurements, Paris, pp. 125–132.

Craft, T.J., Launder, B.E., Suga, K., 1995. A non-linear eddy-viscosity model including sensitivity to stress anisotropy. In: Proceedings of the Tenth Symposium on Turbulent Shear Flows. Pennsylvania State University, pp. 23.19–23.24.

Craft, T.J., Launder, B.E., Suga, K., 1996. Development and application of a cubic eddy-viscosity model of turbulence. Int. J. Heat Fluid Flow 17, 108–115.

Craft, T.J., Launder, B.E., Suga, K., 1997. Prediction of turbulent transitional phenomena with a nonlinear eddy-viscosity model. Int. J. Heat Fluid Flow 18, 15–28.

Daly, B.J., Harlow, F.H., 1970. Transport equation in turbulence. Phys. Fluids 13, 2634–2649.

Gatski, T.B., Speziale, C.G., 1993. On explicit algebraic stress models for complex turbulent flows. J. Fluid Mech. 254, 59–78.

Handler, R.A., Swean Jr., T.F., Leighton, R.I., Swearingen, J.D., 1993. Length scales and the energy balance for turbulence near a free surface. AIAA J. 31, 1988–2007.

Horiuti, K., 1990. Higher-order terms in the anisotropic representation of Reynolds stresses. Phys. Fluids A 2, 1708–1710.

Horiuti, K., 1993. Scalar transport in a fully developed 2-D channel flow. In: Kasagi, N. (Ed.), Establishment of the Direct Numerical Simulation Data Bases of Turbulent Transport Phenomena – DNS Database revised in 1993. Mech. Eng. Univ. of Tokyo, Japan.

Kader, B.A., 1981. Temperature and concentration profiles in fully turbulent boundary layers. Int. J. Heat Mass Transfer 24, 1541–1544.

Kasagi, N., Ohtsubo, Y., 1993. Direct numerical simulation of low Prandtl number thermal fluid in a turbulent channel flow. In: Durst, F. et al. (Eds.), Turbulent Shear Flows, vol. 8. Springer, Berlin, pp. 97–119.

Kim, J., 1990. In: Bradshaw, P. et al. (Eds.), 1990. The Collaborative Testing of Turbulence Models. Data disk No. 4.

Kim, J., Moin, P., 1989. Transport of passive scalars in a turbulent channel flow. In: Andre, J.-C. et al. (Eds.), Turbulent Shear Flows, vol. 6. Springer, Berlin, pp. 85–96.

Kim, J., Moin, P., Moser, R., 1987. Turbulence statistics in fully developed channel flow at low Reynolds number. J. Fluid Mech. 177, 133–166.

Kuroda, A., Kasagi, N., Hirata, M., 1995. Direct numerical simulation of turbulent plane Couette–Poiseuille flows: effect of mean shear rate on the near wall turbulence structures. In: Durst, F. et al. (Eds.), Turbulent Shear Flows, vol. 9. Springer, Berlin, pp. 241–257.

Launder, B.E., 1975. On the effects of a gravitational field on the turbulent transport of heat and momentum. J. Fluid Mech. 67, 569–581.

Launder, B.E., 1976. Heat and mass transport. In: Bradshaw, P. (Ed.), Topics in Applied Physics, vol. 12. Turbulence. Springer, Berlin, pp. 231–287.

Launder, B.E., 1988. On the computation of convective heat transfer in complex turbulent flows. ASME J. Heat Transfer 110, 1112–1128.

Launder, B.E., Reynolds, W.C., 1983. Asymptotic near-wall stress dissipation rates in a turbulent flow. Phys. Fluids 26, 1157–1158.

Launder, B.E., Tselepidakis, D.P., 1993. Contribution to the modelling of near-wall turbulence. In: Durst F. et al. (Eds.), Turbulent Shear Flows, vol 8. Springer, Berlin, pp. 81–96.

Leschziner, M.A., 1982. An introduction and guide to PASSABLE. UMIST Mech. Eng. Rep. TF/82/11.

Lombardi, P., DeAngelis, V., Banerjee, S., 1996. Direct numerical simulation of near-interface turbulence in coupled gas-liquid flow. Phys. Fluids 8, 1643–1665.

Lumley, J.L., 1978. Computational modeling of turbulent flows. Adv. Appl. Mech. 18, 123–176.

Myong, H.K., Kasagi, N., 1990. Prediction of anisotropy of the near wall turbulence with an anisotropic low-Reynolds number $k - -\varepsilon$ turbulence model. ASME J. Fluid Eng. 112, 521–524.

Neumann, J.C., 1968. Transfert de chaleur en régime turbulent pour les grands nombres de Prandtl. Inform. Aéraul. et Therm. 5, 4–20.

Nezu, I., Rodi, W., 1986. Open-channel flow measurements with a laser-Doppler anemometer. J. Hydraulic Engng. 112, 335–355.

Nisizima, S., Yoshizawa, A., 1987. Turbulent channel and Couette flows using an anisotropic k–ε. AIAA J. 25, 414–420.

Pope, S., 1975. A more general effective-viscosity hypothesis. J. Fluid Mech. 72, 331–340.

Pope, S., 1983. Consistent modelling of scalars in turbulent flows. Phys. Fluids 26, 404–408.

Rhee, G.H., Sung, H.J., 1997. A low-Reynolds-number, four-equation heat transfer model for turbulent separated and reattaching flows. Int. J. Heat Fluid Flow 18, 38–44.

Rodi, W., 1980. Turbulence models and their application in hydraulics. International Association of Hydraulic Research Delft (1993 third ed. Balkema Rotterdam).

Rogers, M.M., Mansour, N.N., Reynolds, W.C., 1989. An algebraic model for the turbulent flux of a passive scalar. J. Fluid Mech. 203, 77–101.

Rubinstein, R., Barton, J.M., 1990. Non-linear Reynolds stress models and renormalization group. Phys. Fluids A 2, 1472–1476.

So, R.M.C., Sommer, T.P., 1995. An explicit algebraic heat-flux model for the temperature field. Int. J. Heat Mass Transfer 39, 455–465.

Speziale, C.G., 1987. On nonlinear k–l and k–ε models of turbulence. J. Fluid Mech. 178, 459–475.

Suga, K., 1995. Development and application of a non-linear eddy viscosity model sensitized to stress and strain invariants. Ph.D. thesis, UMIST, Manchester, UK.